Technical Report No. 42

DROUGHT AT THE GLOBAL SCALE IN THE 2ND PART OF THE 20TH CENTURY (1963-2001)

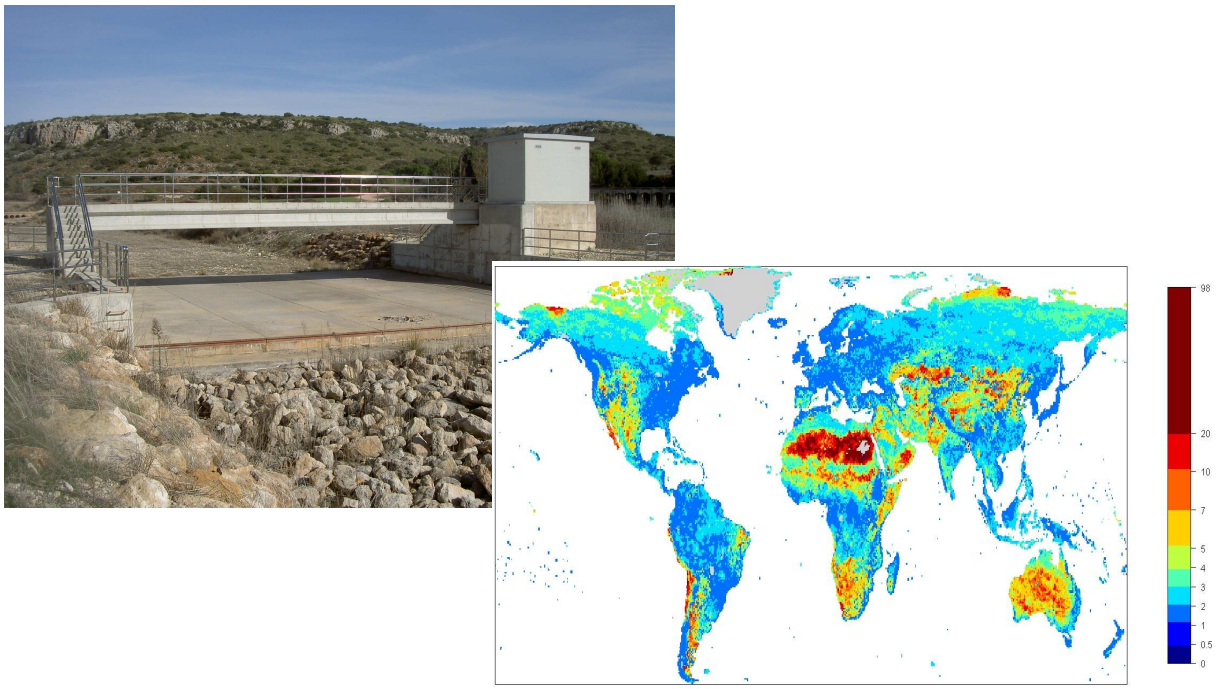

Marjolein van Huijgevoort, Pieter Hazenberg, Henny van Lanen, Nathalie Bertrand, Douglas Clark, Sonja Folwell, Sandra Gomes, Simon N. Gosling, Naota Hanasaki, Jens Heinke, Sujan Koirala, Tobias Stacke & Frank Voβ

August 2011

WATCH is an Integrated Project Funded by the European Commission under the Sixth Framework Programme, Global Change and Ecosystems Thematic Priority Area (contract number: 036946).
The WATCH project started 01/02/2007 and will continue for 4 years.

Title:	Drought at the global scale in the 2nd part of the 20th Century (1963-2001)
Authors:	Marjolein van Huijgevoort, Pieter Hazenberg, Henny van Lanen Nathalie Bertrand, Douglas Clark, Sonja Folwell, Sandra Gomes, Simon N. Gosling, Naota Hanasaki, Jens Heinke, Sujan Koirala, Tobias Stacke & Frank Voβ
Organisations:	- Wageningen University - Hydrology and Quantitative Water Management Group (WUR) - Laboratoire de Météorologie Dynamique (LMD), France - Centre for Ecology and Hydrology, UK - Centro de Geofisica da Universidade de Lisboa, Portugal - University of Nottingham, UK - National Institute for Environment Studies, Japan - Potsdam-Institute for Climate Impact Research, Germany - University of Tokyo, Japan - Max Planck Institute for Meteorology, Germany - University of Kassel, Germany
Submission date:	August 2011
Function:	This report is an output from Work Block 4; Task 4.1.1 Investigate processes controlling the propagation of drought, and Task 4.1.2 Spatial and temporal scales and severity of droughts in 20th century.
Deliverable	WATCH deliverables D 4.1.4 Report on the increased understanding of the propagation of drought in different hydro-climatological regions, physical catchment structures and different scales, D 4.1.3a Methodologies to quantify the space-time development of droughts at regional and continental scales, and it contributes to M4.1-3 Space time development and propagation of drought: comparison of regions derived from LSHMs, and M4.1-6 Overview of major historical events; part: drought.

Photo cover: Left: dry streamflow gauging station in the Upper-Guadiana Basin (2008)
Right: average drought duration (months) derived from the simulated runoff with the large-scale model MPI-HM

Summary

The large impacts of drought on society, economy and environment urge for a thorough investigation. A good knowledge of past drought events is important for both understanding of the processes causing drought, as well as to provide reliability assessments for drought projections for the future. Preferably, the investigation of historic drought events should rely on observations. Unfortunately, for a global scale these detailed observations are often not available. Therefore, the outcome of global hydrological models (GHMs) and off-line land surface models (LSMs) is used to assess droughts. In this study we have investigated to what extent simulated gridded time series from these large-scale models capture historic hydrological drought events. Results of ten different models, both GHMs and LSMs, made available by the WATCH project, were compared. All models are run on a global 0.5° grid for the period 1963-2000 with the same meteorological forcing data (WATCH forcing data). To identify hydrological drought events, the monthly aggregated total runoff values were used. Different methods were developed to identify spatio-temporal drought characteristics.

General drought characteristics for each grid cell, as for example the average drought duration, were compared. These characteristics show that when comparing absolute values the models give substantially different results, whereas relative values lead to more or less the same drought pattern. Next to the general drought characteristics, some documented major historical drought events (one for each continent) were selected and described in more detail. For each drought event, the simulated drought clusters (spatial events) and their characteristics are given for one month during the event. It can be concluded that most major drought events are captured by all models. However, the spatial extent of the drought events differ substantially between the models. In general the models show a fast reaction to rainfall and therefore also capture drought events caused by large rainfall anomalies. More research is still needed, since here we only looked at a few selected number of documented drought events spread over the globe. To assess more in detail if these large-scale models are able to capture drought, additional quantitative analyses are needed together with a more elaborated comparison against observed drought events.

Contents

1 Introduction

Drought is a natural hazard that occurs all over the world, because of climate variability. It is also one of the least understood natural hazards (Wilhite, 2000). This is partly due to the fact that drought develops slowly and imperceptibly and may therefore remain unnoticed for a long time (Tallaksen & van Lanen, 2004). Drought can have large economic, social and environmental impacts. The consequences and costs of drought are difficult to estimate due to the regionally extensive occurrence and the fact that drought affects many different sectors, which cannot all be put in economic numbers (Markandya *et al.*, 2009). Published data on the economic costs of drought usually refer to one sector, one region and one year (EurAqua, 2004). Data for Europe from 2000 to 2006 show that each year on average 15% of the EU total area and 17% of the EU total population have suffered from the impact of droughts (European Commission, 2006). The total cost of droughts over the past 30 years amounts to 100 billion Euros (European Commission, 2007). One recent severe drought in Europe occurred in 2003 and spread over a large area. More than 30.000 people died from the associated heat wave.

The large impacts of drought on the society, economy and environment urge for a thorough investigation of drought processes. This is even more important because drought is likely to become more extreme in many places of the world due to global change (e.g. Bates *et al.* (2008)). Past drought events have to be well understood to identify adequate drought projections. The space-time development, distribution and occurrence of drought events in the past century have been studied at different spatial scales e.g. catchment (Hisdal & Tallaksen, 2003; Peters *et al.*, 2006; Tallaksen *et al.*, 2009), regional (Hisdal *et al.*, 2001; Sheffield *et al.*, 2004; Andreadis *et al.*, 2005; Shukla & Wood, 2008; Bordi *et al.*, 2009; Stahl *et al.*, 2010; Wong *et al.*, 2011) and global scale (Fleig *et al.*, 2006; Sheffield & Wood, 2007; 2008; Dai *et al.*, 2009; Sheffield *et al.*, 2009). Preferably, the investigation of historic drought events should rely on observations, but only few large-scale studies do (e.g. Bordi *et al.* (2009); Wilson *et al.* (2010); Prudhomme *et al.* (2011); Stahl *et al.* (2011); Wong *et al.* (2011)). Most studies predominantly use (global) hydrological models and off-line land surface models to assess drought and very often in a single model context, although it is anticipated that models deviate in outcome and against observations (e.g. Prudhomme *et al.* (2011); Stahl *et al.* (2011)).

This study intercompares global hydrological drought in a multi-model setting. The multi-model experiments of the EU-funded WATCH project (www.eu-watch.org) provide the opportunity for such analyses (Haddeland *et al.*, 2011). We used a subset of the WATCH model ensemble (i.e. 10 large-scale models) with the aim to explore to what extent the models capture historic hydrological drought events (Fig. 1). Some models are classified as global hydrological models (GHMs), whereas others belong to the off-line land surface models (LSMs). All 10 models were run over the period 1963-2000 on a global 0.5 degree grid and forced by the same weather data obtained from the WATCH Forcing Data (WFD, Weedon *et al.* (2011)).

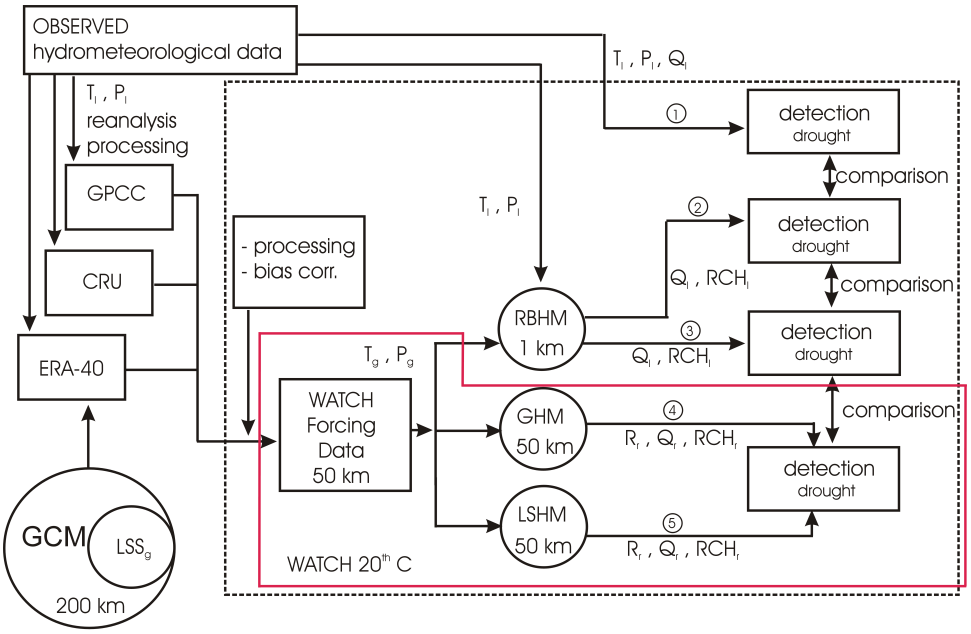

Figure 1: Flow chart showing the context of the multi-model intercomparison of large-scale models for the second part of the 20th century within WATCH. The red box indicates the data used in this study.

First we will briefly summarize the main properties of the suite of large-scale models (GHMs and LSMs) that has been used in this study, followed by a description of the common forcing data (WFD) and the drought identification approach (Chapter 2). Then we will present the global distribution of average duration of drought in runoff as an example of a general drought characteristic. Maps of all ten large-scale models will be presented. We also will intercompare the number of land grids that have a large number of days with zero runoff. Next we will present for each continent a major documented drought event and how this has been simulated with the different large-scale models. We will use spatial drought clusters and some of their properties (e.g. area, centroid) to describe agreement among the models (Chapter 3). Finally, we will draw some conclusions.

2 Methodology and data

The multi-model analysis is carried out with ten different large-scale models, both Land Surface Models (LSMs) and Global Hydrological Models (GHMs). The models used in this study are described below. The drought analysis is done using monthly aggregated runoff time series of these models. The method for drought analysis is also given below.

2.1 Large-scale models

Through the EC-FP6 project WATCH (Water and Global CHange) results from different large-scale models are available. In this multi-model analysis ten models are used: H08, HTESSEL, JULES, Orchidee, MATSIRO (LSMs) and WaterGAP, MPI-HM, LPJml, GWAVA, MacPDM (GHMs). We followed the division in subgroups proposed by Haddeland *et al.* (2011). In Table 1 some characteristics for each of the models are given.
All models have the same model setup and forcing data, as described in detail by Haddeland *et al.* (2011). All models use the land mask defined by CRU (Climate Research Unit), resulting in a resolution of 0.5° x 0.5° for land points only (67420 cells). They were run for a 43-year period (1958-2000), of which the first 5-years were used as spin-up period (1958-1962). Human impacts such as reservoir operation and water withdrawals for agriculture or drinking water were not included. In this study we focused on hydrological drought at the global scale. Therefore, we have used the time series of total runoff (sum of surface runoff Qs and subsurface runoff Qsb). The runoff values are available at a daily time step, however for the drought analysis the daily simulated runoff values were aggregated up to a monthly scale. Aggregating was performed to minimize the impact of too flashy model simulations. Next to that, it can be expected that the impact of a major drought event, as opposed to a flood event, is still observable at the monthly time scale due to its long duration and slow response.

2.2 Forcing data

The meteorological forcing data for all models were the WATCH Forcing Data (WFD) developed by Weedon *et al.* (2010; 2011), but the time step and meteorological variables used, differ between the models (Table 1). The WFD consist of gridded time series of meteorological variables (e.g. rainfall, snowfall, temperature, wind speed) both on a subdaily and daily basis for 1958-2001. The data have a resolution of 0.5° x 0.5°. The WFD originate from modification (bias-correction and downscaling) of the ECMWF ERA-40 re-analysis data, which are subdaily data on a one-degree spatial resolution (Uppala *et al.*, 2005). The different weather variables have been interpolated and corrected for elevation differences between the ERA-40 one degree elevations and the CRU half-degree elevations. For precipitation, the ERA-40 data were firstly adjusted to have the same number of wet (i.e. rain- or snow-) days as the CRU wet day data. Next, the data were bias corrected using monthly GPCC precipitation totals (Schneider *et al.*, 2008) and finally, gauge-catch corrections were applied separately for rainfall and snowfall. Additionally, the interpolated ERA-40 near-surface temperatures were elevation corrected and bias-corrected using both CRU monthly average temperatures and CRU monthly average diurnal temperature ranges. For more information the reader is referred to Weedon *et al.* (2010; 2011).

Table 1: Main characteristics of the participating models (derived from Haddeland *et al.* (2011))

Model name[a]	Model timestep	Meteorological forcing variables[b]	Energy balance	Evapotranspiration scheme[c]	Runoff scheme[d]	Snow scheme	Reference(s)
GWAVA	Daily	P, T, W, Q, LWn, SW, SP	No	Penman-Monteith	Saturation excess/Beta function	Degree day	(Meigh *et al.*, 1999)
H08	6 h	R, S, T, W, Q, LW, SW, SP	Yes	Bulk formula	Saturation excess/Beta function	Energy balance	(Hanasaki *et al.*, 2008)
HTESSEL	1 h	R, S, T, W, Q, LW, SW, SP	Yes	Penman-Monteith	Variable infiltration capacity/ Darcy	Energy balance	(Balsamo *et al.*, 2009)
JULES	1 h	R, S, T, W, Q, LW, SW, SP	Yes	Penman-Monteith	Infiltration excess/ Darcy	Energy balance	(Best *et al.*, 2011; Clark *et al.*, 2011)
LPJmL	Daily	P, T, LWn, SW	No	Priestley-Taylor	Saturation excess	Degree day	(Bondeau *et al.*, 2007; Rost *et al.*, 2008)
MacPDM	Daily	P, T, W, Q, LWn, SW	No	Penman-Monteith	Saturation excess/Beta function	Degree day	(Arnell, 1999; Gosling & Arnell, 2011)
MATSIRO	1 h	R, S, T, W, Q, LW, SW, SP	Yes	Bulk formula	Infiltration and saturation excess/ Groundwater	Energy balance	(Takata *et al.*, 2003; Koirala, 2010)
MPI-HM	Daily	P, T	No	Thornthwaite	Saturation excess/Beta function	Degree day	(Hagemann & Gates, 2003; Hagemann & Dümenil, 1998)
Orchidee	15 min	R, S, T, W, Q, SW, LW, SP	Yes	Bulk formula	Saturation excess	Energy balance	(de Rosnay & Polcher, 1998)
WaterGAP	Daily	P, T, LWn, SW	No	Priestley-Taylor	Beta function	Degree day	(Alcamo *et al.*, 2003)

[a] Model names written in bold are classified as LSMs in this paper; the other models are classified as GHMs.

[b] R: Rainfall rate, S: Snowfall rate, P: Precipitation (rain or snow distinguished in the model), T: air temperature, W: Wind speed, Q: Specific humidity, LW: Longwave radiation flux (downward), LWn: Longwave radiation flux (net), SW: Shortwave radiation flux (downward), SP: Surface pressure

[c] Bulk formula: Bulk transfer coefficients are used when calculating the turbulent heat fluxes.

[d] Beta function: Runoff is a nonlinear function of soil moisture.

2.3 Drought analysis

The following section presents a short overview of the implementations which have been performed to identify whether within a given region of the world, a drought occurs for a given time step. Two different steps are presented. First, it is explained how one is able to asses whether within a given half-degree grid cell a drought occurs. It can be expected a drought event is larger than an individual cell. Therefore, at the global scale a clustering analysis was implemented as well, which is able to identify multiple cells corresponding to the same drought region. The main benefit of this method is that, since the clustering method is performed for different drought severities, it provides information about the spatial impact of the drought at possibly multiple impact levels.

2.3.1 Temporal drought identification

Two different methods were implemented to derive hydrological drought from the modelled time series, the threshold level method and the consecutive dry period (CDP) approach. For situations where runoff values are larger than zero, the threshold level method (Yevjevich, 1967; Hisdal *et al.*, 2004) is used. With this method, a drought occurs when the variable of interest (e.g. streamflow, precipitation, recharge) is below a predefined threshold (Fig. 2). The start of a drought event is indicated by the point in time when the variable falls below the threshold and the event continues until the threshold is exceeded again. Drought characteristics commonly derived with this method are beginning, end, duration, deficit volume, and minimum flow during

an event (Hisdal *et al.*, 2004; Fleig *et al.*, 2006). Both a fixed and variable (seasonal, monthly, or daily) threshold can be used (Hisdal *et al.*, 2004). In this study a monthly threshold is used.

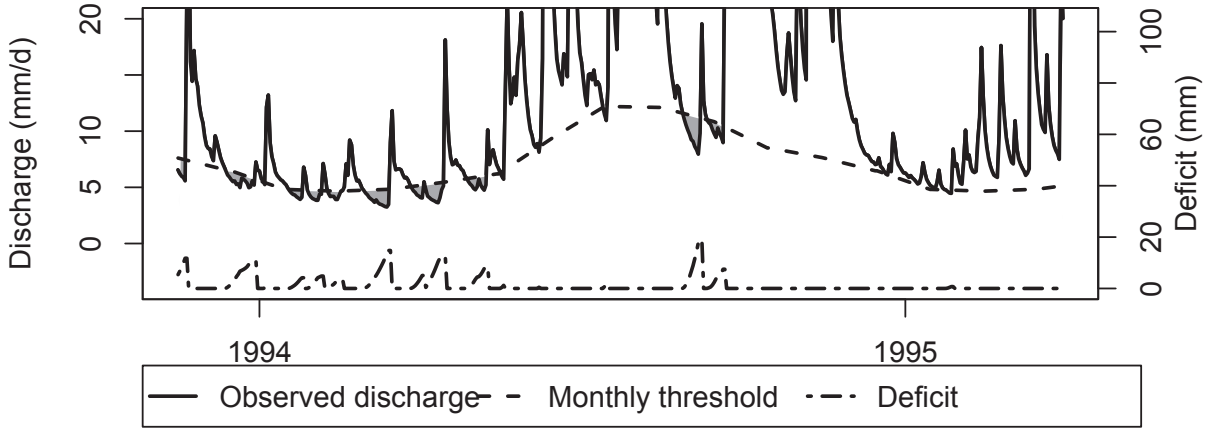

Figure 2: Threshold level method with a variable (monthly) threshold (Van Huijgevoort *et al.* (2010) data from Tallaksen & van Lanen (2004)).

Unfortunately, the threshold approach has difficulties to make a distinction between a drought and a normal situation for regions where zero runoff is observed during part of the year, either because precipitation occurs in the form of snow (winter period in higher latitudes) or is not observed at all (arid and semi-arid regions). Therefore, for cells which have a zero runoff for at least 5% of their time series, a consecutive dry period (CDP) approach was developed. This technique is related to the consecutive dry day approach originally developed to study meteorological drought (Vincent & Mekis, 2006; Groisman & Knight, 2008; Deni & Jemain, 2009). In its current implementation, this method is combined with the threshold level method applied to positive runoff data. An implementation of the CDP approach is presented in Fig. 3. The runoff time series plotted in Fig. 3a contains multiple periods with zero runoff. The first step is to apply the threshold method, to identify months that are in drought but still contain positive runoff values (Fig. 3a). Based on this information, two different series are identified. The first contains the consecutive number of months with zero runoff (Fig. 3b, red line), while the second contains the number of consecutive months for a pixel either being in a drought (based on the threshold method) or containing zero runoff. Based on all data in the first series and the threshold of interest, one is able to calculate a consecutive number threshold value for a given exceedence interval (Fig. 3b, dashed line). This consecutive number threshold value is compared to the second series, which contains both the threshold level method and zero runoff information. In case the monthly value of that second series is larger as compared to the consecutive number threshold value for a month with zero runoff data, the pixel experiences a drought.

In the space-time analysis of drought and the comparison with major historical drought events, several exceedance percentiles (Q80, Q85, Q90, Q95) were derived from the flow duration curve. In this study, for instance, the Q80 is defined as the flow that is equaled or exceeded in 80% of the time. It was decided to use multiple percentile levels, in order to be able to assess the severity of a drought within a spatial event, as well. Comparison between the different models with respect to their general drought characteristics was performed with the monthly Q80 threshold. The Q80 value was selected in order to be consistent with other global and large scale studies (e.g. Sheffield *et al.* (2009); Andreadis *et al.* (2005)). This value is an indication of low flows rather than focusing on severe drought events only.

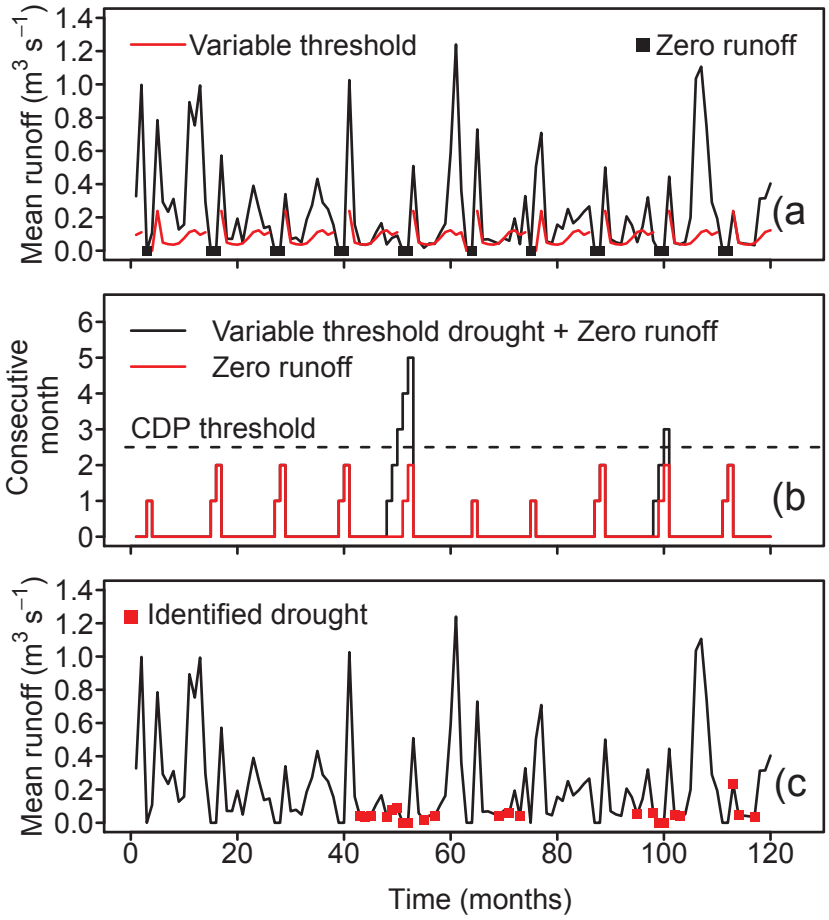

Figure 3: Drought identification approach for a given exceedence interval. a) gives the variable threshold method. Black dots indicate months with zero runoff. Red line in b) shows the consecutive number of months with zero runoff from which a threshold can be calculated based on a given exceedence interval (dashed line). In case the consecutive number of dry months, which are either in drought based on a) or that have zero runoff, is larger than this consecutive threshold value, a drought is observed during the month with zero runoff. The final result of identified months experiencing a drought is plotted in c.

2.3.2 Spatial drought identification

As explained before, it can generally be expected that, in case a drought is observed, this will encompass multiple individual half-degree grid cells. In literature, multiple techniques have been developed to cluster individual cells in drought. The most straightforward method to perform such a cluster identification is to join neighbouring cells. Andreadis *et al.* (2005) applied a recursion-based approach to link a given cell, which is in a drought, to its eight neighbours. Even though this method is easy to implement, recursion-based approaches consume lots of computing power. Next to that, recursion-based approaches are impossible to implement in a hierarchical manner. Therefore, if one wants to implement a clustering scheme which is able to assess drought for different percentile levels, one has to repeat this analysis multiple times, before one is able to link these drought regions hierarchically, which again increases computation time.

In this study, it was therefore decided not to implement a recursion-based approach. Especially since the focus here lies on identifying drought clusters at the global scale.
The current study implemented a top-down divisive deterministic clustering algorithm using a connected component technique. The general ideas behind connected component techniques were originally developed by Rosenfeld & Pfaltz (1966) and Rosenfeld (1970). This approach makes it possible to discriminate within a given drought region, multiple subregions for which the simulated drought is more intense, in a fast and straightforward manner.
To focus only on major spatial drought events, an areal threshold was included (Tallaksen *et al.*, 2009; Sheffield *et al.*, 2009). This areal threshold differs for each percentile, for the 80^{th} percentile the areal threshold is 25 grid cells (approximately 62 500 km^2). The higher the monthly threshold, the smaller the areal threshold becomes, because the severity of the drought increases with the percentile.

3 Results

3.1 General drought characteristics

For each of the models the drought characteristics are determined separately for each cell over the globe. In some cells the threshold level method is used, in other cells a combination of the CDP approach and threshold level method (Section 2.3.1) . In most models there are also cells which never have runoff, e.g. in the Sahara and Greenland. These cells are completely excluded from all analyses, the number of cells which do not have runoff are given in Table 2 (last column) for each model. Table 2 also gives an overview of the number of cells in which the CDP approach is used in the different models. These numbers differ substantially between the models, this is caused by the different way models implement storage and, associated to that, how they react to rainfall. Very fast reacting models, like LPJml, have much more cells with zero runoff than slowly reacting models like MacPDM. There is a distinction between the LSMs (top five models Table 2) and the GHMs, all LSMs have a similar number of cells with the combined CDP approach, while the GHMs give a much lower number of cells, except LPJml. However, runoff can be very small in the models with very limited number of cells with zero runoff (e.g. GWAVA) in for example arid regions.

One of the calculated drought characteristics is the average duration. Fig. 4 shows the results for all models. The average duration is given for each cell and is presented in percentiles of the total range of average durations of all cells for a particular model to account for large differences in absolute values among the models (Appendix A). For example, if a particular cell has got the colour green it implies that the cell has an average drought duration that is in the range of the 40-60% percentile of the average drought duration of all cells. So at least 40% of the cells of that particular model have a longer average drought duration.

Cells that do not have droughts in the entire time series (e.g. part of the Sahara) are given in gray. In the calculation of the average drought characteristics, droughts that started in the first timestep or do not end before the time series ends, are not taken into account. Therefore, there can be more cells without droughts in the analysis than cells without runoff. GWAVA, for example, simulates time series in parts of the Sahara which slowly drop during the entire time series. Too high initial conditions or one rainfall event in the beginning of this time series could cause this behaviour. This will always lead to a drought at the end of the time series, because that is where the lowest runoff values occur. Since this drought does not end within the time series, it is not taken into account when calculating the average drought duration. Cells with this phenomena are thus given in gray here. However, in the spatial drought analysis (Section 3.2), drought areas are calculated separately for each time step, in which case these cells are taken into account and can become part of a drought cluster.

All models give, as expected, a long average duration in the driest areas of the world, e.g. the Sahara, only the extent of this area differs between the models. Most of the models also agree on short average duration in areas with a high runoff. These areas have a high variability in runoff which leads to many, short droughts e.g. the Amazon catchment. Large differences are visible in the cold arid regions, e.g. Siberia and Alaska, this is caused by the different snow schemes of the models, the difficulties that models encounter when modeling snow processes and the fact that not all models include a glacier scheme (Haddeland *et al.*, 2011). This is also the reason Greenland is excluded from the results of the average drought durations. Other drought characteristics, like total number of drought (Appendix B), give a similar result.

Table 2: Number of cells for each model with CDP approach and zero runoff

Model	# cells CDP approach	# cells without runoff
H08	13942	53
JULES	16421	96
Orchidee	16477	350
HTESSEL	15296	556
MATSIRO	12819	569
WaterGAP	4820	818
LPJml	44990	140
GWAVA	0	74
MPI-HM	4427	3350
MacPDM	0	0

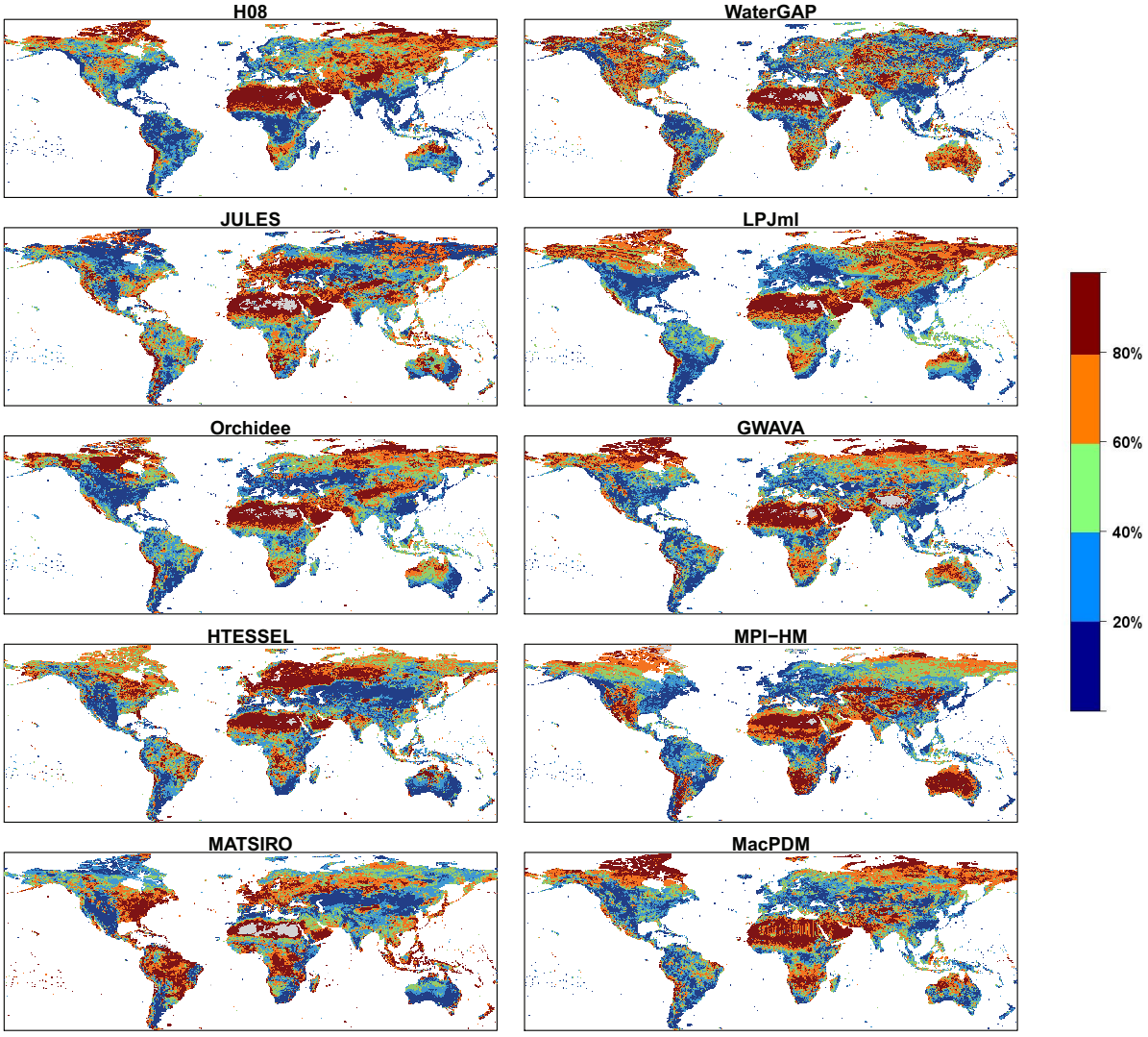

Figure 4: Average duration of droughts presented in percentiles of total range of durations for each global model.

3.2 Spatial drought analysis

To compare simulated drought events with documented major historical drought events, one event is selected for each continent to investigate whether the models are able to reproduce the spatial extent of these events. The major events chosen here are selected based on literature (e.g. Sheffield *et al.* (2009)). For each drought event, the spatial extent of the drought clusters in a particular month are given. Besides the graphical presentation also some characteristics of the clusters at that time step are calculated. For each time step, the total number of clusters spread over the world, the average size of these clusters, the size of the largest cluster (both in real area (km^2) based on the projection of the world and in number of grid cells) and the coordinates of the centroid of the largest cluster are given. Although the months that are shown are based on a drought event in a certain continent, the clusters are given for the whole globe. There might be also substantial drought clusters in other continents in that particular month. These other drought events are also discussed. The drought events are described in chronological order.

3.2.1 South America

In 1963 a drought event with a large spatial extent and long duration occurred in South America (Sheffield *et al.*, 2009). In Table 3 and Fig. 5 the drought clusters for all models and their characteristics are given for October 1963. Almost all models agree on a drought in South America, however the exact spatial extent and location differ. The results of MATSIRO stand out in the figure showing a very large area of the globe in drought. This is exceptional and it is unclear as to why this model gives this result, this could be caused by a too short spin-up period, since the results of MATSIRO deviate from the other model results mainly during the beginning of the time series (see also Section 3.2.2).
Besides the drought in South America, other regions also show large clusters of drought. All models, except MacPDM, give drought in the US and Australia, although especially in Australia the extent and severity differ substantially. The year 1963 is mentioned as the beginning of a multiyear drought in Australia from 1963 to 1968 (BoM, 1997). The fact that this was more or the less at the start of the drought event could cause difference between the models, since they all have different model structures causing faster or slower reactions of the subsurface runoff to the meteorological forcing data.
The 1963 drought in the US is also a known event described in literature (Andreadis *et al.*, 2005). The spatial extent and severity of this event agree quite well in 8 of the ten models (only MATSIRO and MacPDM produce deviant results). These eight models all place the centroid of the largest cluster in the US in this month (Table 3). Although the exact areas of the largest cluster differ, most of these models agree reasonably well. The H08 model gives a larger area in the US compared to the rest, however looking at the spatial extents given in Fig. 5 this model does not stand out. Probably the other models are dividing the drought in the US in two or more clusters with only a small number of non-drought cells in between them, while for the H08 model these cells are all connected. This could be prevented by using a different threshold of the division of clusters, so that more than only neighbouring cells are taken into account when identifying the clusters.
Overall, most models agree that at this timestep there were three large drought events spread over the globe, with the drought in the US having the largest spatial extent.

Table 3: Characteristics of low flow clusters across the globe in October 1963

Model	# clusters	Average size 10^4 km^2	Average size # cells	Area max cluster 10^4 km^2	Area max cluster # cells	Centroid largest cluster lon (°)	Centroid largest cluster lat (°)
H08	69	49.3	215	751.2	3054	-89.25	45.25
JULES	81	34.5	152	498.5	2271	-87.75	44.25
Orchidee	84	34.5	140	438.6	1884	-84.25	41.75
HTESSEL	79	35.6	149	540	2452	-93.25	44.25
MATSIRO	54	127.1	644	2124.8	11591	-168.75	52.25
WaterGAP	66	35.4	155	537.4	2395	-87.75	42.75
LPJml	58	53.7	208	594.1	2675	-87.75	43.75
GWAVA	72	36.2	150	560.3	2523	-87.25	43.75
MPI-HM	73	39.5	164	580.3	2580	-87.75	42.75
MacPDM	61	29.6	120	453.5	1555	-58.25	-17.75

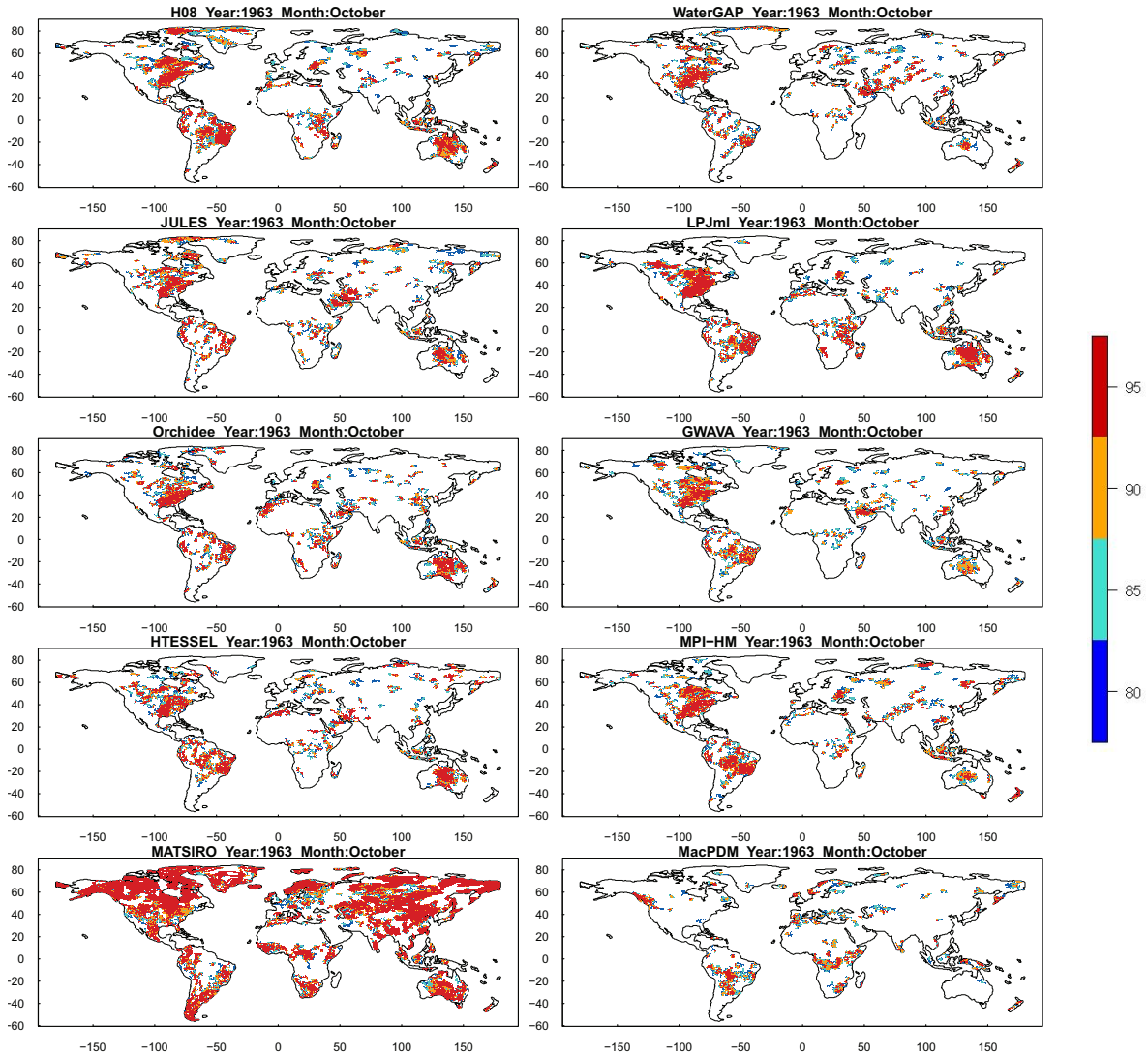

Figure 5: Spatial distribution of low flow clusters with runoff below a number of thresholds (80, 85, 90 and 95 percentile) derived from all models for October 1963

3.2.2 Australia

In Table 4 and Fig. 6 drought clusters are given for the month January in 1965. In the period 1963-1968 a large part of Australia experienced a severe multiyear drought (BoM, 1997). This month gives a snapshot of that drought. From Fig. 6 and Table 4 it is clear that most models have more or less a comparable average size in clusters (except MATSIRO), and also a comparable number of clusters. MATSIRO, as mentioned before (Section 3.2.1), stands out with a very large area of the globe in drought.
Most of the models (7 out of ten) agree on the location of the largest drought cluster in this month and place it in the middle of Australia. Although all models agree on a large drought in this part of the world, the drought in Australia is represented differently by each model when looking at the spatial extent.
Besides the drought in Australia, all models give other, smaller areas in drought spread across the world. However, there is less agreement between the models about the occurrence and extent of these events.

Table 4: Characteristics of low flow clusters across the globe in January 1965

Model	#	Average size		Area max cluster		Centroid largest cluster	
	clusters	10^4 km^2	# cells	10^4 km^2	# cells	lon (°)	lat (°)
H08	71	39.9	188	636.1	2300	133.75	-25.75
JULES	73	32.2	137	426.7	1544	135.25	-26.25
Orchidee	77	28.9	128	592.6	2163	133.25	-27.25
HTESSEL	79	27.5	122	538.5	1947	135.25	-25.75
MATSIRO	60	59.1	334	861.6	4950	-107.75	55.25
WaterGAP	81	25.2	117	406.8	1434	132.25	-22.75
LPJml	51	36.0	144	641.3	2329	133.75	-26.25
GWAVA	75	25.8	115	433.7	1542	134.25	-24.25
MPI-HM	69	32.2	146	403.9	2010	96.75	57.25
MacPDM	44	50.8	209	384.2	1367	-64.25	-22.25

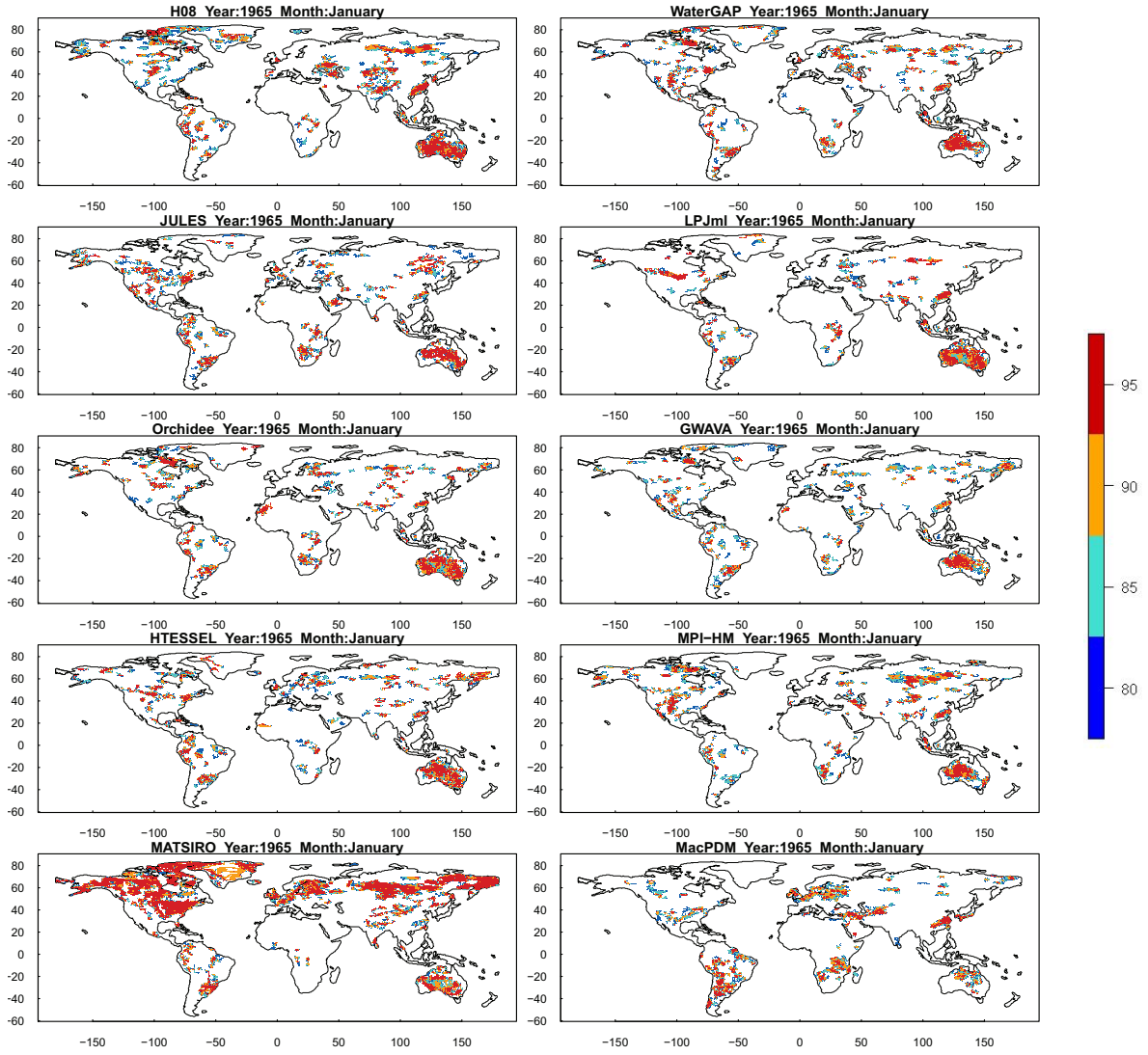

Figure 6: Spatial distribution of low flow clusters with runoff below a number of thresholds (80, 85, 90 and 95 percentile) derived from all models for January 1965

3.2.3 Europe

In 1976 a long period of lower than normal rainfall, beginning in autumn 1975, caused a severe and widespread drought in Europe (Zaidman *et al.*, 2002; Stahl, 2001). In June and July 1976 the drought event reached its maximum spatial extent. Most affected areas were Western Europe and the UK spreading to Central Europe and later on to Northern Europe (Zaidman *et al.*, 2002; Stahl, 2001). The models all agree on a drought event in July 1976 (Fig. 7), and, apart from Orchidee and LPJml, they show a very similar spatial extent corresponding to the areas mentioned in literature. Less agreement can be found in the other drought events captured by the models, some give large events in Australia, others in the US. Table 5 also shows this; the coordinates of the centroid of the largest cluster differ between the models. Six models (JULES, HTESSEL, MATSIRO, WaterGAP, GWAVA, MacPDM) place the largest cluster in Europe and they also give more or less the same area in drought for the maximum cluster.

Table 5: Characteristics of low flow clusters across the globe in July 1976

Model	#	Average size		Area max cluster		Centroid largest cluster	
	clusters	10^4 km^2	# cells	10^4 km^2	# cells	lon (°)	lat (°)
H08	73	39.0	184	506.2	1851	130.75	-27.25
JULES	92	26.1	125	292.9	1614	15.25	53.75
Orchidee	90	23.4	112	235.2	895	82.25	64.25
HTESSEL	85	26.7	125	415.8	2334	24.25	54.75
MATSIRO	68	28.8	141	337.0	1826	16.75	53.25
WaterGAP	89	27.1	128	354.2	2009	16.25	54.75
LPJml	80	29.6	132	359.8	1328	129.75	-28.25
GWAVA	77	26.0	120	284.3	1614	15.25	54.75
MPI-HM	79	25.9	122	230.5	1214	94.25	62.75
MacPDM	74	34.2	155	323.3	1752	14.75	53.25

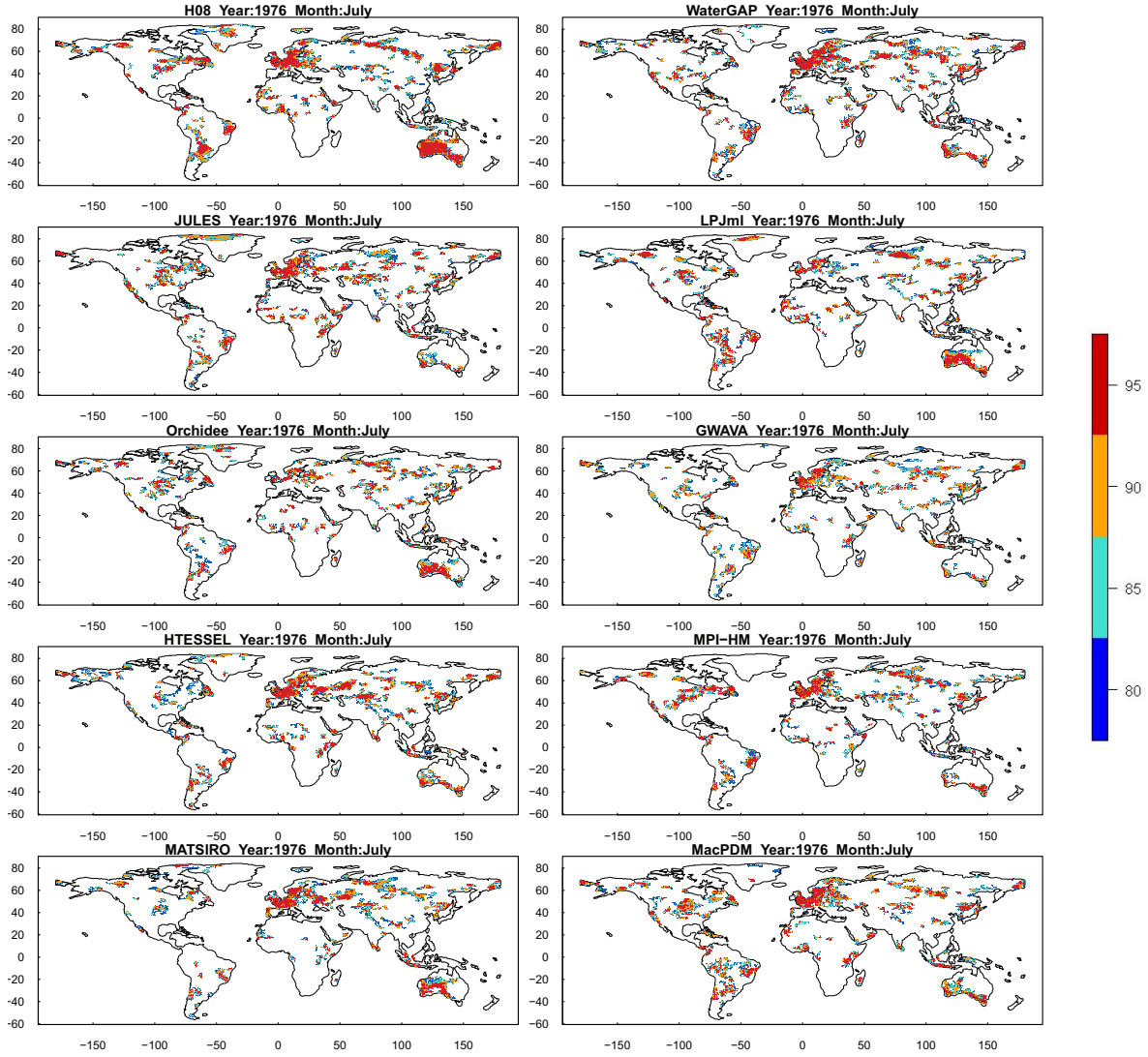

Figure 7: Spatial distribution of low flow clusters with runoff below a number of thresholds (80, 85, 90 and 95 percentile) derived from all models for July 1976

3.2.4 Africa

In the 1980s large parts of Africa suffered from drought, one well-known event is a drought in the Sahel in 1983-1984 (Dai *et al.*, 2004; Sheffield *et al.*, 2009; Dai, 2011). This event was caused by very low rainfall in the Sahel that followed after a major El Ñino event in 1982-83 (Dai *et al.*, 2004). According to Sheffield *et al.* (2009), this drought event spread over Africa and reached its maximum extent in April 1983. Therefore Table 6 and Fig. 8 show drought clusters and their characteristics for this particular month from all models. From Fig. 8 it can be concluded that all models pick up on a drought event in the Sahel. Most models also extent the drought into Southern Africa. Overall there is a good agreement on the spatial extent of the drought in the Sahel between the models and also with the area in drought as given by Sheffield *et al.* (2009).
However, the models also simulate drought in other parts of the world, which explains why the coordinates of the centroid of the maximum cluster differ between the models. Besides the drought in the Sahel (5 models locate the largest cluster there), large droughts are simulated in Southern Africa (WaterGAP, MPI-HM and MacPDM place the maximum cluster there). When models agree on the spatial location of the largest cluster, the area of the largest cluster they give is also very similar. All models also agree on drought in South America, especially in the northwest part. Part of Indonesia is suffering from drought according to all models, but not as widespread as in 1997 (Section 3.2.6). These areas where drought is simulated are all influenced again by the major El Ñino event of 1982-83 mentioned by Dai *et al.* (2004), although in this particular month not as severe as in October 1997 (Section 3.2.6).

Table 6: Characteristics of low flow clusters across the globe in April 1983

Model	# clusters	Average size 10^4 km^2	Average size # cells	Area max cluster 10^4 km^2	Area max cluster # cells	Centroid largest cluster lon (°)	Centroid largest cluster lat (°)
H08	71	43.3	193	642.1	2195	4.75	14.75
JULES	76	29.8	123	270.8	885	3.75	6.75
Orchidee	82	28.9	134	211.4	689	3.75	5.75
HTESSEL	78	32.1	139	276.4	902	4.75	6.25
MATSIRO	74	24.5	116	311.0	1010	-54.25	-2.25
WaterGAP	92	33.3	147	336.7	1170	24.75	-20.75
LPJml	56	60.0	271	597.8	3667	99.25	57.75
GWAVA	82	29.5	130	228.2	745	2.75	6.25
MPI-HM	69	43.5	180	324.9	1137	23.75	-21.25
MacPDM	87	33.8	151	369.4	1292	24.75	-21.25

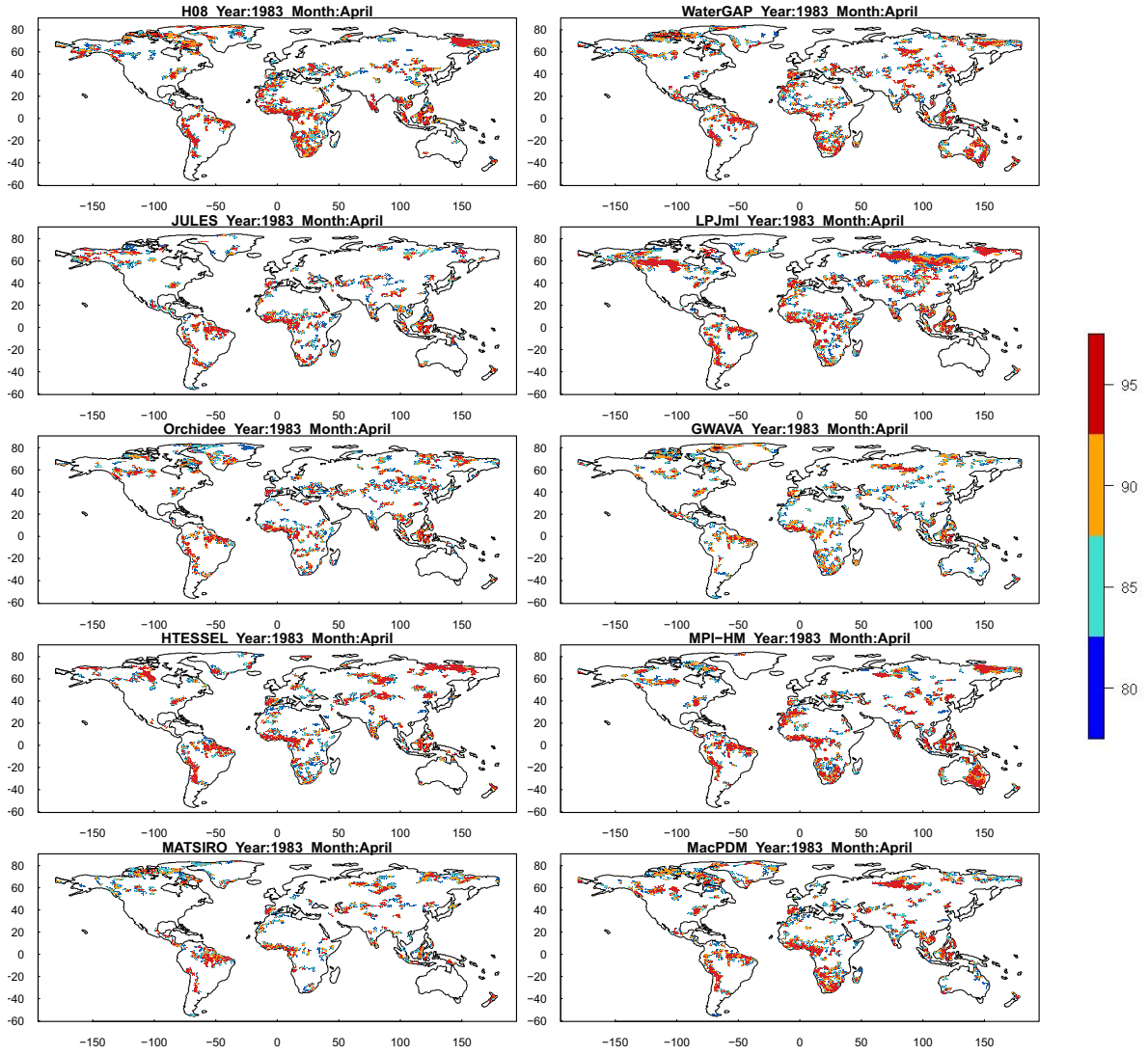

Figure 8: Spatial distribution of low flow clusters with runoff below a number of thresholds (80, 85, 90 and 95 percentile) derived from all models for April 1983

3.2.5 North America

In 1988 a severe drought occurred in the United States, leading to an estimated $30 billion in agricultural losses and contributing to 10 000 deaths from heat stress according to Trenberth & Branstator (1992). This drought event was caused by extreme low rainfall in April, May and June 1988. The meteorological drought ended in July, when rainfall returned to normal or even above normal conditions. However, dry soil conditions, heat waves and hydrological drought continued in July and August. Regions most affected were the Great Plains, the Mid West and the Lower Mississippi Valley (Trenberth & Branstator, 1992). In Table 7 and Fig. 9 the drought clusters simulated by all models are given for July 1988. All models simulate drought in the United States. Most models, except for LPJml and Orchidee, also more or less agree on the spatial extent and locate the drought in the areas that were mentioned by Trenberth & Branstator (1992). The small spatial extent of the drought given by LPJml could be caused by the way a model reacts to rainfall. If this reaction is very fast, the hydrological drought could be ended by the model in July, because rainfall also returned to normal conditions in this month. The spatial extent as given by most of the models is fairly similar to the ones given by Andreadis *et al.* (2005) and Sheffield *et al.* (2009) for June 1988. Six models place the largest spatial cluster of this month in the US, however the maximum area of this largest cluster differs between about 225 and 560*10^4 km^2 (Table 7). Some models have divided this drought event in several clusters (see JULES and Orchidee).
Further, all models agree on a drought event in parts of Russia, some place the largest cluster there. A drought event in (southern) South America is also given by all models. This drought in South America corresponds with a drought event found by Sheffield & Wood (2007) in southern South America in 1988 and is linked to a La Niña event.

Table 7: Characteristics of low flow clusters across the globe in July 1988

Model	#	Average size		Area max cluster		Centroid largest cluster	
	clusters	10^4 km^2	# cells	10^4 km^2	# cells	lon (°)	lat (°)
H08	68	34.3	178	310.9	1799	63.75	61.25
JULES	75	27.2	131	232.9	1067	-100.75	44.75
Orchidee	79	25.4	125	228.2	1054	-91.75	45.25
HTESSEL	75	30.4	145	451.7	2037	-93.25	43.75
MATSIRO	73	25.8	128	253.2	1195	64.25	61.75
WaterGAP	75	31.6	149	455.5	2078	-95.25	44.75
LPJml	68	30.3	156	208.6	1382	64.75	60.75
GWAVA	66	30.4	146	320.6	1691	56.25	60.75
MPI-HM	80	32.4	150	395.4	1785	-96.75	43.75
MacPDM	61	41.1	198	561.3	2585	-92.75	45.25

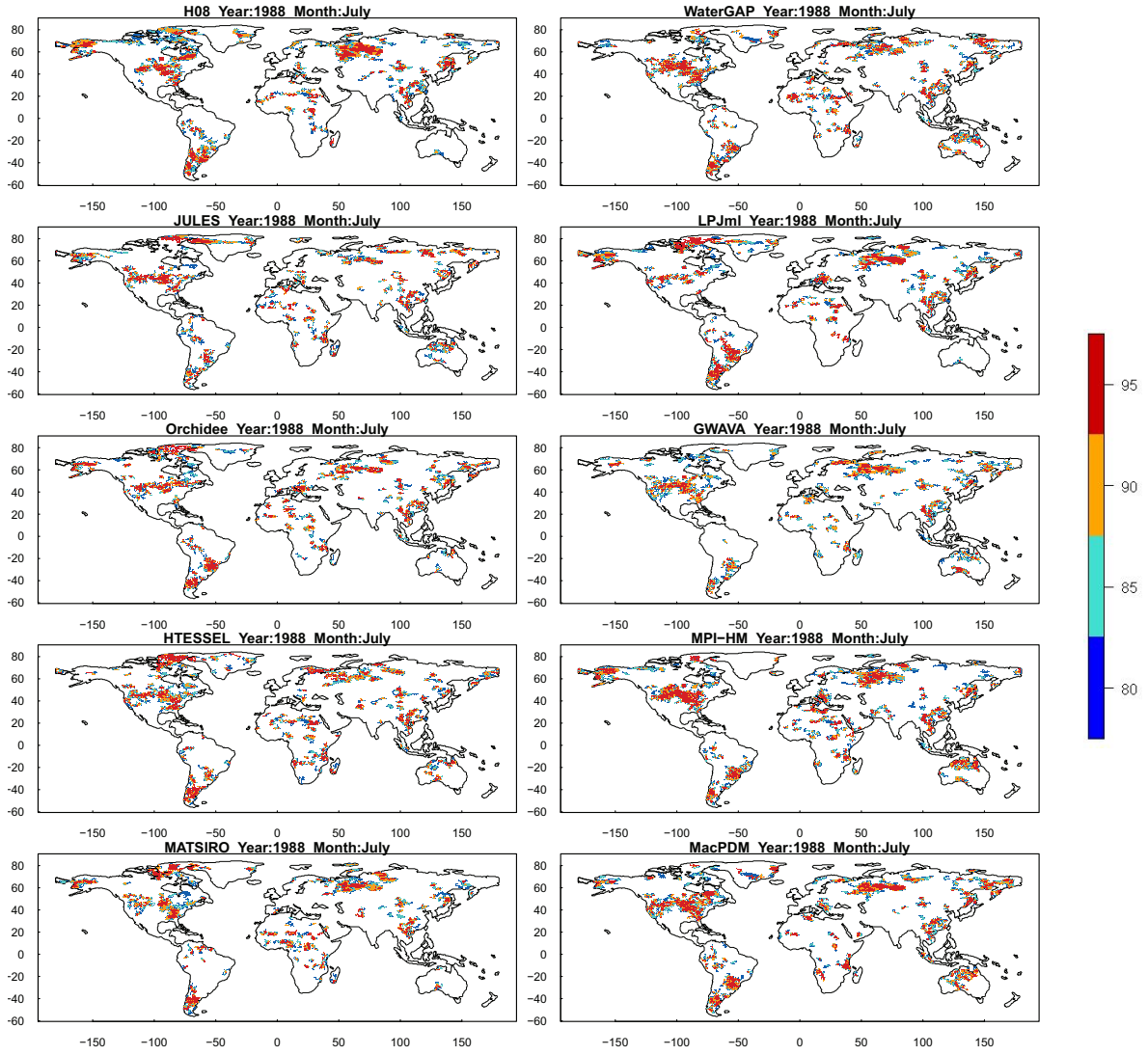

Figure 9: Spatial distribution of low flow clusters with runoff below a number of thresholds (80, 85, 90 and 95 percentile) derived from all models for July 1988

3.2.6 Asia

Drought clusters and their characteristics in October 1997 are shown in Table 8 and Fig. 10. Sheffield *et al.* (2009) indicate that the drought of 1997-98 had the largest spatial extent in Asia. In Fig. 10 it can be observed that all models indeed show drought in Asia, more specifically, in large parts of China and the Indonesian Archipel and its surroundings. The 1997 drought in China was not the most severe drought within China in the last years according to Dai (2011), but is given as an extreme drought. All models show multiple clusters within China. Some clusters are merged by some of the models leading to a larger spatial extent.
Besides the drought in Asia, all models also give an extreme event in the Amazon and some give drought in the Sahel region. Both these drought events and the one in Indonesia are linked to the El Ñino Southern Oscillation (ENSO) and are known major historical events (Bell & Halpert, 1998; Tomasella *et al.*, 2011). The influence of ENSO was very strong in 1997, leading to very low water levels in the Amazon region and large forest fires in Indonesia (Bell & Halpert, 1998; Tomasella *et al.*, 2011). All models seem to agree well on the spatial extent of both the drought events in the Amazon and in Indonesia. A drought event is also visible in all models in Western Africa (e.g. area around the Congo river). Some models also include the Sahel. There is a relation between the drought in the Sahel and ENSO (Bell & Halpert, 1998), for the other regions this is less well documented for the year 1997.
Most models agree well on the average size of the clusters spread over the globe and the number of clusters, an exception is GWAVA which has a larger average size of the clusters. Because a couple of large events occur across the globe in this particular month, the models give different locations for the centroid of the largest cluster (Table 8). From the ten models, four have the largest cluster somewhere in China, while five models locate the largest cluster in the Amazon. GWAVA is the only one with the largest cluster in Africa. Since the location differs between the models, also the area of the largest cluster is different. However, when models agree on the location, the area of the largest cluster is very similar between these models.

Table 8: Characteristics of low flow clusters across the globe in October 1997

Model	#	Average size		Area max cluster		Centroid largest cluster	
	clusters	10^4 km^2	# cells	10^4 km^2	# cells	lon (°)	lat (°)
H08	64	46.8	205	663.9	3027	91.75	44.25
JULES	72	34.3	139	415.2	1358	-64.25	-2.25
Orchidee	69	39.5	171	419.5	1371	-65.25	-2.75
HTESSEL	69	41.2	185	647.3	2817	93.75	41.75
MATSIRO	71	40.0	175	539.8	2354	95.25	41.75
WaterGAP	67	40.9	177	391.8	1274	-62.75	0.25
LPJml	58	41.5	167	460.8	1506	-64.75	-2.75
GWAVA	56	59.4	271	754.6	2571	15.25	14.75
MPI-HM	64	49.1	211	591.0	1930	-62.75	-2.75
MacPDM	70	48.8	218	733.6	2944	92.75	41.25

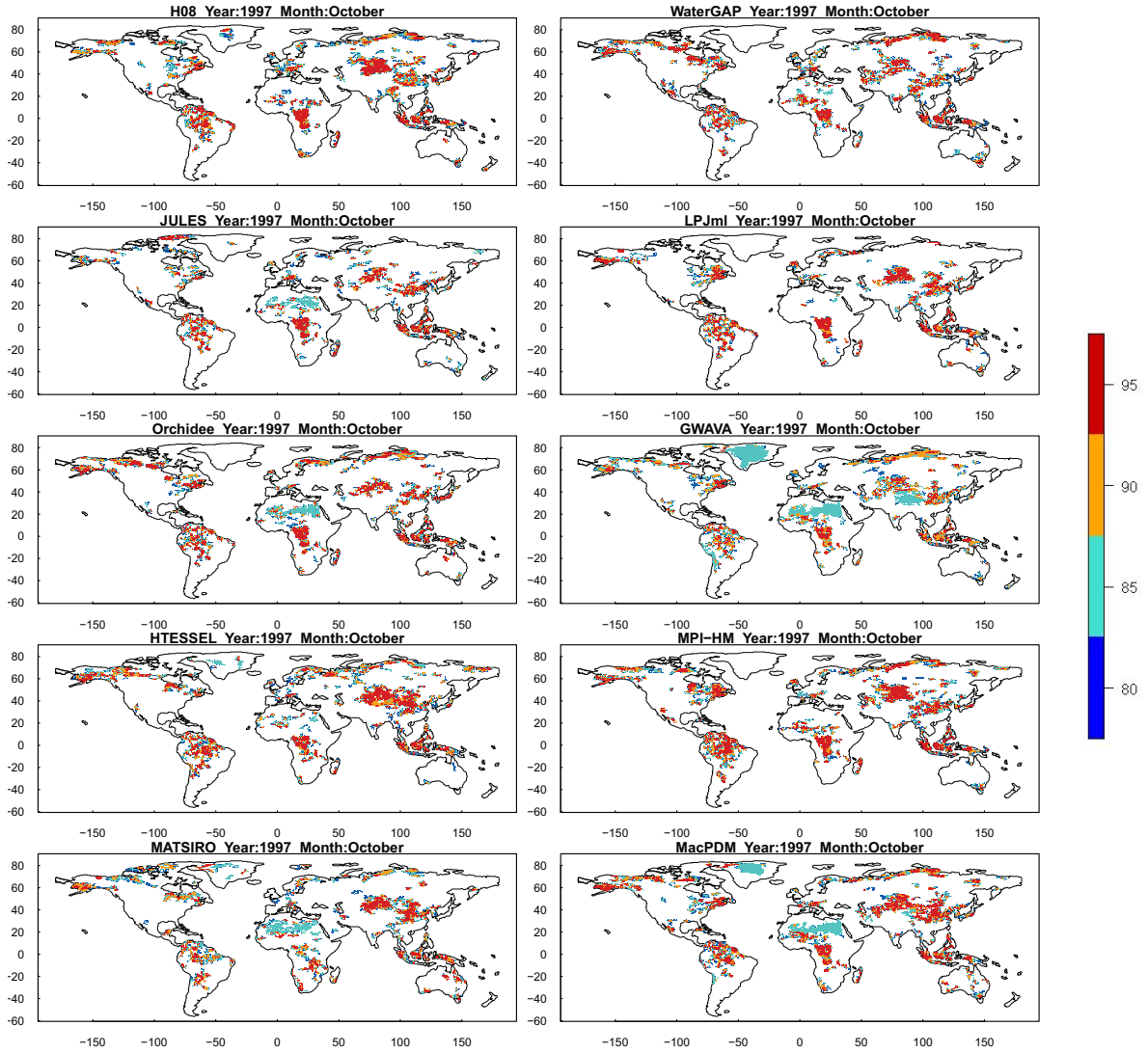

Figure 10: Spatial distribution of low flow clusters with runoff below a number of thresholds (80, 85, 90 and 95 percentile) derived from all models for October 1997

4 Concluding remarks

In this study, we have explored to what extent GHMs and LSMs are able to capture historic hydrological drought events. Results of ten different models that were run over the period 1963-2000 with the same meteorological forcing data, were investigated. General drought characteristics, like the average drought duration for each grid cell, were compared. These characteristics show that the models give substantially different results, when comparing absolute values. Looking at relative values a similar drought pattern between the models is observed. Areas with a high runoff, and thus also a high variability in runoff, have many short drought events. In contrast the driest areas in the world only have a few drought events of very long duration. Largest differences between the average duration occur in cold arid regions.
Besides the general drought characteristics, some documented major historical drought events (one for each continent) were selected and described in more detail. For each drought event, the simulated spatial drought clusters and their characteristics were shown for one particular month during the event. From these figures and tables it can be concluded that most major drought events are captured by all models. However, the spatial extent of the drought events differs substantially between the models. In general, the models show a fast response to rainfall and therefore also mainly capture drought events caused by large rainfall anomalies. This was also found in smaller catchments, see van Loon *et al.* (2011). Drought events related to ENSO are also captured quite reliable by the models because of this fast reaction. However, some drought events may end too soon in some models (e.g. LPJml), because they return to normal conditions as soon as normal rainfall is observed, while in reality hydrological drought often continues after the meteorological drought ends, because stores need to be replenished first. The implementation of these storage processes is model dependent and therefore the spatial extent of drought events can be very different between the models.
More research is still needed, since here we only looked at a few selected number of drought events spread over the globe. To assess more in detail if these large-scale models are able to capture drought, more quantitative analyses are needed and a more elaborated comparison against observed drought events.

References

Alcamo, J., Doll, P., Henrichs, T., Kaspar, F., Lehner, B., Rosch, T., & Siebert, S. 2003. Development and testing of the WaterGAP 2 global model of water use and availability. *Hydrological Sciences Journal-Journal Des Sciences Hydrologiques*, **48**(3), 317–337.

Andreadis, K. M., Clark, E. A., Wood, A. W., Hamlet, A. F., & Lettenmaier, D. P. 2005. Twentieth-century drought in the conterminous United States. *Journal of Hydrometeorology*, **6**(6), 985–1001.

Arnell, NW. 1999. A simple water balance model for the simulation of streamflow over a large geographic domain. *Journal of Hydrology*, **217**(3-4), 314–335.

Balsamo, G., Viterbo, P., Beljaars, A., van den Hurk, B., Hirschi, M., Betts, A. K., & Scipal, K. 2009. A Revised Hydrology for the ECMWF Model: Verification from Field Site to Terrestrial Water Storage and Impact in the Integrated Forecast System. *Journal of Hydrometeorology*, **10**(3), 623–643.

Bates, B.C., Kundzewicz, Z.W., Wu, S., & Palutikof, J.P. 2008. *Climate Change and Water*. Technical Paper of the Intergovernmental Panel on Climate Change, Intergovernmental Panel on Climate Change, Geneva.

Bell, GD, & Halpert, MS. 1998. Climate assessment for 1997. *Bulletin of the American Meteorological Society*, **79**(5), S1–S50.

Best, M. J., Pryor, M., Clark, D. B., Rooney, G. G., Essery, R .L. H., Ménard, C. B., Edwards, J. M., Hendry, M. A., Porson, A., Gedney, N., Mercado, L. M., Sitch, S., Blyth, E., Boucher, O., Cox, P. M., Grimmond, C. S. B., & Harding, R. J. 2011. The Joint UK Land Environment Simulator (JULES), model description - Part 1: Energy and water fluxes. *Geoscientific Model Development*, **4**(3), 677–699.

BoM. 1997. *Living with Drought*. http://www.bom.gov.au/climate/drought/livedrought.shtml. Australian Bureau of Meteorology. accessed: 07-2011.

Bondeau, A., Smith, P. C., Zaehle, S., Schaphoff, S., Lucht, W., Cramer, W., & Gerten, D. 2007. Modelling the role of agriculture for the 20th century global terrestrial carbon balance. *Global Change Biology*, **13**(3), 679–706.

Bordi, I., Fraedrich, K., & Sutera, A. 2009. Observed drought and wetness trends in Europe: an update. *Hydrology and Earth System Sciences*, **13**(8), 1519–1530.

Clark, D. B., Mercado, L. M., Sitch, S., Jones, C. D., Gedney, N., Best, M. J., Pryor, M., Rooney, G. G., Essery, R. L. H., Blyth, E., Boucher, O., Harding, R. J., Huntingford, C., & Cox, P. M. 2011. The Joint UK Land Environment Simulator (JULES), model description - Part 2: Carbon fluxes and vegetation dynamics. *Geoscientific Model Development*, **4**(3), 701–722.

Dai, A, Lamb, PJ, Trenberth, KE, Hulme, M, Jones, PD, & Xie, PP. 2004. The recent Sahel drought is real. *International Journal of Climatology*, **24**(11), 1323–1331.

Dai, A. G., Qian, T. T., Trenberth, K. E., & Milliman, J. D. 2009. Changes in Continental Freshwater Discharge from 1948 to 2004. *Journal of Climate*, **22**(10), 2773–2792.

Dai, Aiguo. 2011. Drought under global warming: a review. *Wiley Interdisciplinary Reviews-Climate Change*, **2**(1), 45–65.

de Rosnay, P, & Polcher, J. 1998. Modelling root water uptake in a complex land surface scheme coupled to a GCM. *Hydrology and Earth System Sciences*, **2**(2-3), 239–255.

Deni, Sayang Mohd, & Jemain, Abdul Aziz. 2009. Mixed log series geometric distribution for sequences of dry days. *Atmospheric Research*, **92**(2), 236–243.

EurAqua. 2004. Towards a European Drought Policy. *Discussion document. EurAqua Secretariat, CEH, Wallingford, UK.*

European Commission. 2006. *Water Scarcity and Drought First Interim Report.*

European Commission. 2007. *Communication Addressing the challenge of water scarcity and droughts in the European Union, (COM(2007) 414).*

Fleig, A. K., Tallaksen, L. M., Hisdal, H., & Demuth, S. 2006. A global evaluation of streamflow drought characteristics. *Hydrology and Earth System Sciences*, **10**(4), 535–552.

Gosling, Simon N., & Arnell, Nigel W. 2011. Simulating current global river runoff with a global hydrological model: model revisions, validation, and sensitivity analysis. *Hydrological Processes*, **25**(7), 1129–1145.

Groisman, Pavel Ya., & Knight, Richard W. 2008. Prolonged dry episodes over the conterminous united states: New tendencies emerging during the last 40 years. *Journal of Climate*, **21**(9), 1850–1862.

Haddeland, Ingjerd, Clark, Douglas B., Franssen, Wietse, Ludwig, Fulco, Voss, Frank, Arnell, Nigel W., Bertrand, Nathalie, Best, Martin, Folwell, Sonja, Gerten, Dieter, Gomes, Sandra, Gosling, Simon N., Hagemann, Stefan, Hanasaki, Naota, Harding, Richard, Heinke, Jens, Kabat, Pavel, Koirala, Sujan, Oki, Taikan, Polcher, Jan, Stacke, Tobias, Viterbo, Pedro, Weedon, Graham P., & Yeh., Pat. 2011. Multi-Model Estimate of the Global Terrestrial Water Balance: Setup and First Results. *Journal of Hydrometeorology*, **early online release**(0). doi: 10.1175/2011JHM1324.1.

Hagemann, S., & Dümenil, L. 1998. A parametrization of the lateral waterflow for the global scale. *Climate Dynamics*, **14**(1), 17–31.

Hagemann, S, & Gates, LD. 2003. Improving a subgrid runoff parameterization scheme for climate models by the use of high resolution data derived from satellite observations. *Climate Dynamics*, **21**(3-4), 349–359.

Hanasaki, N., Kanae, S., Oki, T., Masuda, K., Motoya, K., Shirakawa, N., Shen, Y., & Tanaka, K. 2008. An integrated model for the assessment of global water resources Part 1: Model description and input meteorological forcing. *Hydrology and Earth System Sciences*, **12**(4), 1007–1025.

Hisdal, H., & Tallaksen, L. M. 2003. Estimation of regional meteorological and hydrological drought characteristics: a case study for Denmark. *Journal of Hydrology*, **281**(3), 230–247.

Hisdal, H., Stahl, K., Tallaksen, L. M., & Demuth, S. 2001. Have streamflow droughts in Europe become more severe or frequent? *International Journal of Climatology*, **21**(3).

Hisdal, H., Tallaksen, L. M., Clausen, B., Peters, E., & Gustard, A. 2004. Hydrological Drought Characteristics. *Pages pp. 139–198 of:* Tallaksen, L. M., & van Lanen, H.A.J. (eds), *Hydrological Drought Processes and Estimation Methods for Streamflow and Groundwater.* Developments in Water Science, 48: Elsevier Science B.V.

Koirala, S. 2010. *Explicit representation of groundwater process in a global-scale land surface model to improve hydrological predictions*. Ph.D. thesis, The University of Tokyo.

Markandya, A., Mysiak, J., Palatnik, R., Breil, M., Balzarolo, P., & Martin-Ortega, J. 2009. *Economic and Social Impacts of Droughts and Demand Side Options - State of the Art Review, Draft Background Document Xerochore*.

Meigh, J. R., McKenzie, A. A., & Sene, K. J. 1999. A grid-based approach to water scarcity estimates for eastern and southern Africa. *Water Resources Management*, **13**(2), 85–115.

Peters, E., Bier, G., van Lanen, H. A. J., & Torfs, Pjjf. 2006. Propagation and spatial distribution of drought in a groundwater catchment. *Journal of Hydrology*, **321**(1-4), 257–275.

Prudhomme, Christel, Parry, Simon, Hannaford, Jamie, Clark, Douglas B., Hagemann, Stefan, & Voss, Frank. 2011. How well do large-scale models reproduce regional hydrological extremes in Europe? *Journal of Hydrometeorology*, **early online release**(0). doi: 10.1175/2011JHM1387.1.

Rosenfeld, A. 1970. Connectivity in digital pictures. *Journal of The ACM*, **17**, 146–160.

Rosenfeld, A., & Pfaltz, J. L. 1966. Sequential operations in digital picture processing. *Journal of The ACM*, **13**(4), 471–494.

Rost, Stefanie, Gerten, Dieter, Bondeau, Alberte, Lucht, Wolfgang, Rohwer, Janine, & Schaphoff, Sibyll. 2008. Agricultural green and blue water consumption and its influence on the global water system. *Water Resources Research*, **44**(9), 1–12.

Schneider, U., Fuchs, T., Meyer-Christoffer, A., & Rudolf, B. 2008. *Global Precipitation Analysis Products of the GPCC*. (available from reports and publications section of the GPCC homepage - gpcc.dwd.de).

Sheffield, J., & Wood, E. F. 2007. Characteristics of global and regional drought, 1950-2000: Analysis of soil moisture data from off-line simulation of the terrestrial hydrologic cycle. *Journal of Geophysical Research-Atmospheres*, **112**(D17).

Sheffield, J., & Wood, E. F. 2008. Global trends and variability in soil moisture and drought characteristics, 1950-2000, from observation-driven Simulations of the terrestrial hydrologic cycle. *Journal of Climate*, **21**(3), 432–458.

Sheffield, J., Goteti, G., Wen, F. H., & Wood, E. F. 2004. A simulated soil moisture based drought analysis for the United States. *Journal of Geophysical Research-Atmospheres*, **109**(D24).

Sheffield, J., Andreadis, K. M., Wood, E. F., & Lettenmaier, D. P. 2009. Global and Continental Drought in the Second Half of the Twentieth Century: Severity-Area-Duration Analysis and Temporal Variability of Large-Scale Events. *Journal of Climate*, **22**(8), 1962–1981.

Shukla, S., & Wood, A. W. 2008. Use of a standardized runoff index for characterizing hydrologic drought. *Geophysical Research Letters*, **35**(2).

Stahl, K. 2001. *Hydrological Drought - a Study across Europe*. Ph.D. thesis, Albert-Ludwigs-Universität Freiburg, also available from: http://www.freidok.uni-freiburg.de/volltexte/202/, Freiburg, Germany.

Stahl, K., Hisdal, H., Hannaford, J., Tallaksen, L. M., van Lanen, H. A. J., Sauquet, E., Demuth, S., Fendekova, M., & Jodar, J. 2010. Streamflow trends in Europe: evidence from a dataset of near-natural catchments. *Hydrology and Earth System Sciences*, **14**(12), 2367–2382.

Stahl, Kerstin, Tallaksen, Lena M., Gudmundsson, Lukas, & Christensen, Jens H. 2011. Streamflow data from small basins: a challenging test to high resolution regional climate modeling. *Journal of Hydrometeorology*, **early online release**(0). doi: 10.1175/2011JHM1356.1.

Takata, K, Emori, S, & Watanabe, T. 2003. Development of the minimal advanced treatments of surface interaction and runoff. *Global and Planetary Change*, **38**(1-2), 209–222.

Tallaksen, L. M., & van Lanen, H. A. J. (eds). 2004. *Hydrological drought : processes and estimation methods for streamflow and groundwater*. Developments in water science;48, The Netherlands: Elsevier Science BV.

Tallaksen, L. M., Hisdal, H., & van Lanen, H. A. J. 2009. Space-time modelling of catchment scale drought characteristics. *Journal of Hydrology*, **375**(3-4), 363–372.

Tomasella, Javier, Borma, Laura S., Marengo, Jose A., Rodriguez, Daniel A., Cuartas, Luz A., Nobre, Carlos A., & Prado, Maria C. R. 2011. The droughts of 1996-1997 and 2004-2005 in Amazonia: hydrological response in the river main-stem. *Hydrological Processes*, **25**(8), 1228–1242.

Trenberth, KE, & Branstator, GW. 1992. Issues in Establishing Causes of the 1988 Drought over North America. *Journal of Climate*, **5**(2), 159–172.

Uppala, S. M., Kallberg, P. W., Simmons, A. J., Andrae, U., Bechtold, V. D., Fiorino, M., Gibson, J. K., Haseler, J., Hernandez, A., Kelly, G. A., Li, X., Onogi, K., Saarinen, S., Sokka, N., Allan, R. P., Andersson, E., Arpe, K., Balmaseda, M. A., Beljaars, A. C. M., Van De Berg, L., Bidlot, J., Bormann, N., Caires, S., Chevallier, F., Dethof, A., Dragosavac, M., Fisher, M., Fuentes, M., Hagemann, S., Holm, E., Hoskins, B. J., Isaksen, L., Janssen, Paem, Jenne, R., McNally, A. P., Mahfouf, J. F., Morcrette, J. J., Rayner, N. A., Saunders, R. W., Simon, P., Sterl, A., Trenberth, K. E., Untch, A., Vasiljevic, D., Viterbo, P., & Woollen, J. 2005. The ERA-40 re-analysis. *Quarterly Journal of the Royal Meteorological Society*, **131**(612), 2961–3012.

Van Huijgevoort, M.H.J., Van Loon, A.F., Rakovec, O., Haddeland, I., Horácek, S., & Van Lanen, H.A.J. 2010. Drought assessment using local and large-scale forcing data in small catchments. *In: Global Change: Facing Risks and Threats to Water Resources*. IAHS Publ. No. 340.

van Loon, Anne F., van Lanen, Henny A.J., Tallaksen, Lena M., Hanel, Martin, Fendeková, Miriam, Machlica, Andrej, Sapriza, Gonzalo, Koutroulis, Aristeidis, van Huijgevoort, Marjolein H.J., Bermúdez, Jorge Jódar, Hisdal, Hege, & Tsanis, Ioannis. 2011. *Propagation of Drought through the Hydrological Cycle*. Technical Report No. 31. (available at http://www.eu-watch.org).

Vincent, LA, & Mekis, E. 2006. Changes in daily and extreme temperature and precipitation indices for Canada over the twentieth century. *Atmosphere-Ocean*, **44**(2), 177–193.

Weedon, G. P., Gomes, S., Viterbo, P., Shuttleworth, W. J., Blyth, E., Österle, H., Adam, J. C., Bellouin, N., Boucher, O., & Best, M. 2011. Creation of the WATCH Forcing Data and its use to assess global and regional reference crop evaporation over land during the twentieth century. *Journal of Hydrometeorology*, **early online release**(0). doi: 10.1175/2011JHM1369.1.

Weedon, G.P., Gomes, S., Viterbo, P., Österle, H., Adam, J.C., Bellouin, N., Boucher, O., & Best, M. 2010. *The WATCH Forcing Data 1958-2001: a meteorological forcing dataset for land surface- and hydrological-models.* WATCH Technical Report 22. (available at http://www.eu-watch.org).

Wilhite, D.A. (ed). 2000. *DROUGHT A Global Assesment, Vol I &II.* Routledge Hazards and Disasters Series, Routledge, London.

Wilson, Donna, Hisdal, Hege, & Lawrence, Deborah. 2010. Has streamflow changed in the Nordic countries? - Recent trends and comparisons to hydrological projections. *Journal of Hydrology*, **394**(3-4), 334–346.

Wong, Wai Kwok, Beldring, Stein, Engen-Skaugen, Torill, Haddeland, Ingjerd, & Hisdal, Hege. 2011. Climate change effects on spatiotemporal patterns of hydroclimatological summer droughts in Norway. *Journal of Hydrometeorology*, **early online release**. doi: 10.1175/2011JHM1357.1.

Yevjevich, V. 1967. *An objective approach to definition and investigations of continental hydrologic droughts.* Colorado State University.

Zaidman, M. D., Rees, H. G., & Young, A. R. 2002. Spatio-temporal development of streamflow droughts in north-west Europe. *Hydrology and Earth System Sciences*, **6**(4), 733–751.

Appendices

Appendix A

Table I: Absolute values of average drought duration (in months) given for all models for selected percentiles comparable with Fig. 4. This means that 20% of the grid cells has an average drought duration shorter than the absolute value of the 20 percentile, the 100 percentile in this case represents the maximum average duration found for each model.

Model	Percentile				
	20	40	60	80	100
H08	1.8	2	2.3	2.7	93
JULES	1.6	1.9	2.2	2.9	96
Orchidee	1.5	1.8	2.2	2.9	96
HTESSEL	1.7	2.2	2.7	3.3	99
MATSIRO	1.8	2.6	3.3	5	96
WaterGAP	2.3	3.2	4.4	6.4	99
LPJml	1.5	1.8	2.5	2.9	93
GWAVA	2	2.5	3	4	84
MPI-HM	1.8	2.3	3	4.6	98
MacPDM	1.7	2	2.4	3	48

Appendix B

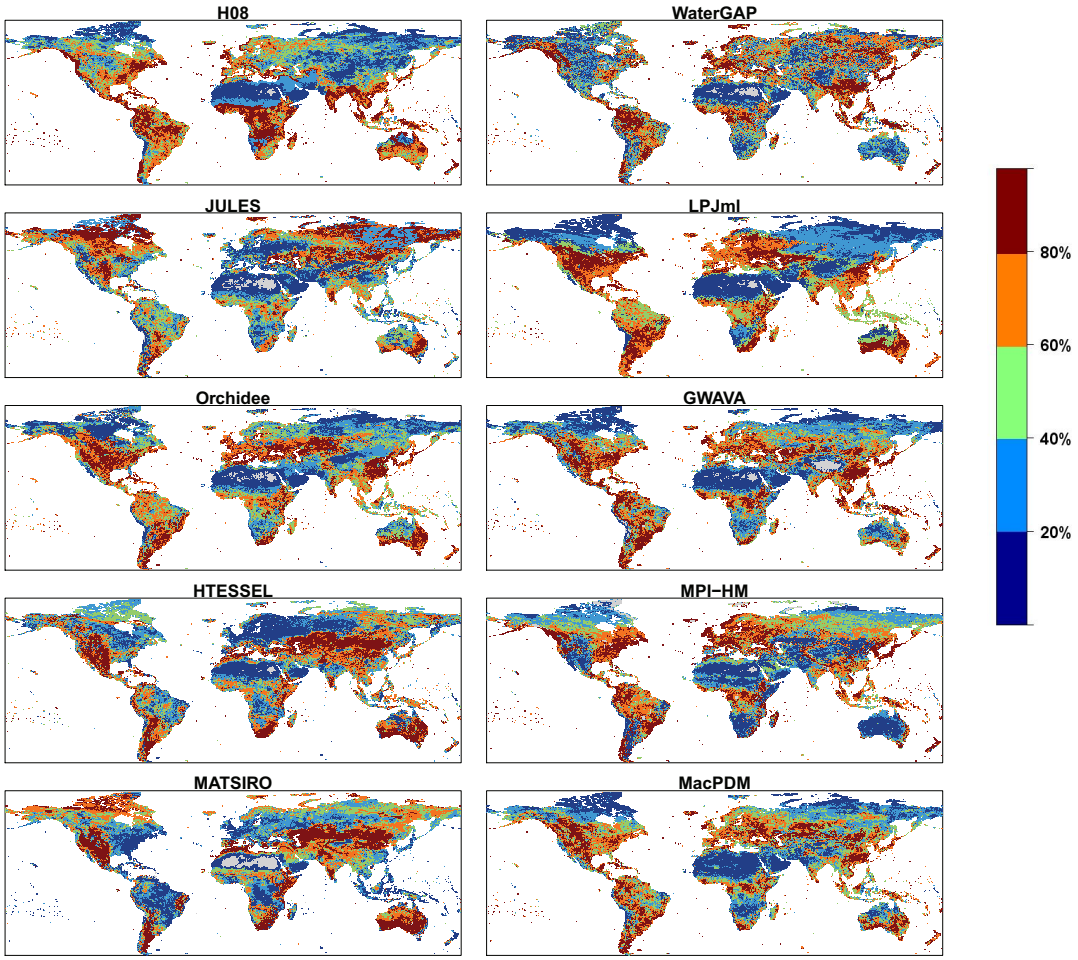

Figure I: Total number of droughts presented in percentiles of total range for each global model

Table II: Absolute values of number of droughts given for all models for selected percentiles comparable with Fig. I

Model	Percentile				
	20	40	60	80	100
H08	36	42	48	55	94
JULES	34	43	52	63	100
Orchidee	35	44	55	68	118
HTESSEL	29	38	45	59	112
MATSIRO	19	29	37	54	131
WaterGAP	15	22	30	42	87
LPJml	38	39	55	65	121
GWAVA	21	28	33	40	80
MPI-HM	21	32	41	53	122
MacPDM	31	39	47	55	89